Influence of mean stress and PWR environment on the fatigue behavior of a 304L austenitic stainless steel

Ziling Peng, Gilbert Hénaff, Jean-Christophe Le Roux, Romain Verlet

INFLUENCE OF MEAN STRESS AND PWR ENVIRONMENT ON THE FATIGUE BEHAVIOR OF A 304L AUSTENITIC STAINLESS STEEL

Ziling Peng[1,2], Gilbert Hénaff[1*], Jean-Christophe Le Roux[2], Romain Verlet[2]

[1]*Pprime Institute, UPR 3346 CNRS ENSMA Université de Poitiers, ISAE-ENSMA, 1 avenue Clément Ader, Futuroscope Chasseneuil, 86961 France, pengziling@mail.iasf.ac.cn*
[2]*EDF, R&D, MMC, Avenue des Renardières – Ecuelles, Moret sur Loing, 77818 France*
[*]: corresponding author: gilbert.henaff@isae-ensma.fr

Abstract

Uni-axial strain-controlled fatigue tests were carried out on a 304L austenitic stainless-steel specimens in air at 300ºC and in PWR water, without or with the application of a mean stress, at different total strain amplitudes. For strain amplitude no less than 0.2%, a deleterious effect of PWR water on fatigue life is observed, associated with the enhancement of both crack initiation and propagation. Besides, the fatigue life is reduced by the application of a mean stress for a fixed strain amplitude in a given environment. In particular, due to the acceleration of crack initiation stage by an enhancement of the plastic strain accumulation, the PWR water effect on fatigue life is re-activated for strain amplitude below 0.2% in the presence of a mean stress. The fatigue life reduction under mean stress application is mostly related to the maximum stress level and strain amplitude, rather than the generated ratcheting strain.

Keywords: crack initiation; crack propagation; ratcheting; environment effect; mean stress;

Nomenclature

a_0 : initial depth of the crack;

C, C_1, C_2 : Paris law coefficients

$\Delta\varepsilon_r$: ratcheting strain;

ΔK_ε : strain intensity factor range ;

$\Delta\varepsilon_t/_2$: Total strain amplitude;

$\varepsilon_{m,\ X\%\ of\ fatigue\ life}$: mean strain measured at X% of the fatigue life;

F_{en} : environmental factor;

$F_{en,theo}$: theoretical value of F_{en};

$F_{en,exp}$: experimental value of F_{en};

$F_{en,semi\text{-}exp}$: semi-experimental value of F_{en};

F_{ms}: mean stress factor;

m, m_1, m_2 : Paris law exponents

$N_{0\ MPa,\ average}$: average fatigue life for tests without mean stress application, for a given strain amplitude and in a given environment;

N_5: fatigue life defined as the number of cycles until the detection of a decrease of 5% with respect to the peak stress measured at mid-life ;

$N_{exp,\ air}$: experimental fatigue life in air;

$N_{exp,\ PWR}$: experimental fatigue life in PWR environment;

$N_{mean,air}$: mean fatigue life in air;

$N_{PWR,\ theo}$: theoretical fatigue life in PWR water;

$N_{0\rightarrow a0}$: number of cycles required to nucleate a crack with a depth of a_0;

$N_{a0\rightarrow 2950\mu m}$: number of cycles required to make a crack grow from an initial depth a_0, to a final depth of 2950 μm;

1. Introduction

Austenitic stainless steels are extensively used in the nuclear industry, thanks to their attractive combination of mechanical properties and corrosion resistance, to manufacture structural components such as primary circuit pipes of Pressurized-Water Reactors (PWR). Nevertheless, the impact of some specific service conditions on the performance of these steels still needs to be addressed in more details in order to assess the conservatism of the design approaches currently used. For instance, between start-up and shutdown operations, these components are subjected to pressure and temperature transient loadings. From a design point of view, such thermal transients are considered equivalent to a strain-controlled fatigue loading to determine the lifetime of the component. Thus, in the ASME code [1] and in the French RCC-M design code [2] , the fatigue life assessment is based on a design curve derived from a broad database of test results obtained under uniaxial strain-controlled cyclic loading in air. Thereafter, different factors are applied to the strain amplitude and to the number of cycles to failure, in order to account for the degradation in fatigue strength induced by various parameters, such as the stress multiaxiality, the size, the surface finishing of the component, or the material variability and the scatter in data. It is worth noticing that, when applying these factors, it is assumed that these parameters influence the fatigue behavior independently from each other, which may lead to a substantial over- or under-conservatism in the life prediction in presence of interactions (synergy or attenuation) [3]. Therefore, the investigation of the effect of these parameters and their interactions is of high interest to improve the accuracy of the fatigue life assessment of nuclear power-plant components.

As more specifically regards the effect of environment, the safety authorities such as NRC in the United States, JNSC in Japan, STUK in Finland or ASN in France, so far request

to take into account the effect of the PWR primary water on the fatigue life of reactor components. This is done on the basis of the fatigue design curve and by considering the F_{en} environmental factor [4]. This factor, defined as the ratio between the fatigue life in air and the fatigue life in PWR environment, is determined by empirical equations as a function of different parameters such as the strain rate, the rate of dissolved oxygen and temperature.

In order to critically assess this type of approach, the possible interactions between environment and other influencing factors such as strain amplitude [5, 6], surface treatments [7-10] [7–], or cold working [11] have been investigated at different temperatures in the recent years. However, it is noteworthy that the vast majority of these studies on the influence of the PWR water were carried out with a total strain amplitude superior to 0.3%. Similar results, but with a lower strain amplitude, are much less documented, albeit in this regime a potentially different balance between the crack initiation stage and the crack propagation stage might justify further investigation. Besides, previous studies were mainly conducted by using alternated tension-compression loadings, with an almost null mean stress. In practice however, in a mixing junction or near a pipe elbow, a thermal stratification of the fluid is likely to develop and to promote a local increase in the mean stress. In literature, the influence of mean stress on fatigue resistance has been investigated, but mainly at room temperature and on the basis of stress-controlled fatigue tests [12-17]. However, recently, Vincent et al. [18] successfully controlled both the strain range and the mean stress to the predefined values by adjusting the mean strain during fatigue tests conducted at ambient temperature. The consequences of this type of loading on the fatigue strength in PWR water are not documented so far, which motivated the present work.

Hence, the research activities undertaken in this study were designed in order to extend the assessment of the influence of PWR water on fatigue behavior of the material, at low total strain amplitudes, typically inferior or equal to 0.2%, but also in presence of an applied mean stress. With this aim, fatigue tests were carried out under total strain-amplitude in air and in PWR environment. Some ancillary tests were interrupted at different stages of the fatigue life in order to derive quantitative assessment of the damage, typically the crack depth. Finally, on the basis of the experimental results, empirical equations were proposed in order to describe the joint effect of total strain amplitude and applied mean stress. The present paper presents the main findings of these investigations.

2. Material, specimens, and testing facilities

A plate of an AISI 304L stainless steel manufactured by Creusot-Loire Industrie (sheet XY182), annealed at 1100 °C and quenched with water is used in this study. The chemical

composition and mechanical properties are presented in Table 1 and in Table 2, respectively. These properties are in good agreement with the RCC-M 3307 requirements [2].

Table 1. Chemical composition (wt. %) of the XY182 material as compared with the requirements of the RCC-M code [2].

Elements	C	Mn	Si	S	Ni	Cr	Mo	Cu
XY182 (%)	0.029	1.86	0.37	0.004	10	18	0.04	0.02
RCC-M (%) M3307	≤ 0.03	≤ 2	≤ 1	≤ 0.03	9 ~ 12	17~20	-	≤ 1

Table 2. Mechanical properties in the rolling direction of 304L austenitic stainless steel [19]

	Rolling direction		Transverse direction		RCC-M M3307 (transverse direction) [12]	
	20°C	300°C	20°C	300°C	20°C	300°C
Yield stress (MPa)	220	138	220	136	≥175	≥105
Ultimate tensile strength (MPa)	555	401	546	402	≥490	-
Elongation (%)	68	48	68	46	≥45	-
Young's Modulus (GPa)	196	168	192	196	-	-

Two different specimen geometries were used in this study, as presented in Fig. 1, namely a tubular hollow geometry designed for tests in PWR environment but that can also be used for testing in air, and a solid cylindrical geometry only used for tests in air. For the hollow specimens, the roughness of the inner and outer surface is $R_{a,in}$=0.2 μm and $R_{a,out}$=0.6 μm, respectively. The analysis of test results has confirmed that the fatal cracks leading to failure systematically initiated from the inner surface. For the solid cylindrical specimens, the surface roughness is R_a=0.2 μm.

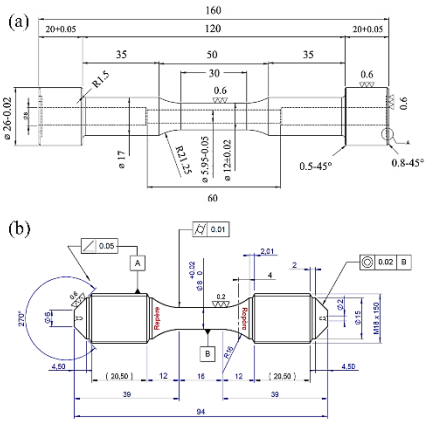

Fig. 1 : Design of the (a) hollow specimen and (b) solid bar specimen (dimensions in mm).

The fatigue tests in PWR primary environment were carried out on an Instron 8862 100kN electromechanical fatigue machine. The hollow specimen is placed in a furnace mounted on the loadframe, and the circulation of the PWR fluid inside the sample in insured by means of a fluid loop while controlling the chemistry of this fluid all along the fatigue test, as illustrated in Fig. 2. The simulated PWR primary water is characterized by 25 cm^3 of dissolved hydrogen per kilogram of water and less than 5 ppb of dissolved oxygen. The conductivity of the high purity inlet and outlet water at 20 ° C is about 21 µS / cm. An extensometer with a gauge length of 12.5 mm placed outside the furnace is used to control the deformation applied to the specimen by means of two ceramic rods in contact with the outer surface of specimen. Prior to the start of the fatigue loading, the furnace is closed, and the loop is heated for at least 24 hours, to ensure an isothermal condition of 300°C in the entire rig.

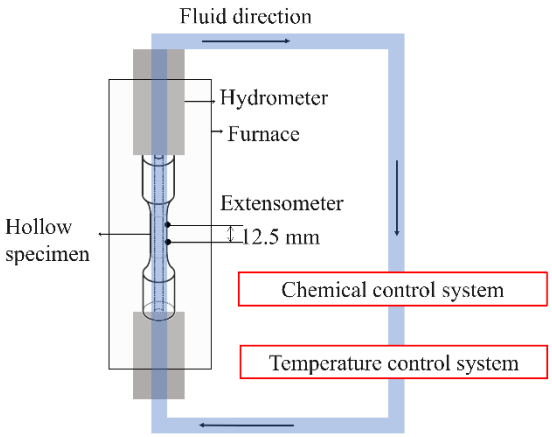

Fig. 2 : Experimental installation for fatigue test in simulated PWR water environment.

Most of the fatigue tests in air were carried out using the same device with the hollow specimen. Besides, due to constraints related to test duration, ancillary fatigue tests at low strain

amplitude were performed in air using solid samples on another INSTRON 8862 100kN electromechanical fatigue machine with an extensometer with a gauge length of 12.5 mm placed outside the furnace, controlling the deformation of the specimen with two ceramic rods in contact with the specimen.

The fatigue life N_5 is defined as the number of cycles applied until the detection of a decrease of 5% with respect to the peak stress measured at mid-fatigue life. In several tests however, such a decrease was not achieved prior to the failure of the specimen or the leak of the fluid through the tube wall. In such cases, the fatigue life was defined as the number of cycles to failure or to the leakage. Uniaxial fatigue experiments were realized under strain-control. A triangular waveshape loading with a strain rate of 0.4% s^{-1} was used. For the test reported here, the imposed total strain amplitude varied from 0.5% to 0.14%. For amplitudes that vary from 0.14% to 0.2%, a tensile mean stress of 20 MPa and 50 MPa was applied in several tests, by means of a tri-modal monitoring method, which is described in more details in section 3.2. Besides, for a strain amplitude of 0.2%, some tests were interrupted after a fixed number of cycles and then conducted to failure by high-cycle fatigue loading in laboratory air at room temperature, with a frequency of 10Hz and a load ratio of 0.2.

3. Results

3.1. Fatigue life without mean stress

The effect of PWR water on fatigue life in the absence of any applied mean stress is illustrated in Fig. 3. In this plot, the dotted blue curve represents the theoretical fatigue life in air as predicted by the mean curve in air proposed in the NUREG report [20], according to Equation 1.

Equation 1 $$N_{mean,air} = \exp\left[6.891-1.92\times\ln\left(\Delta\varepsilon_t/2-0.112\right)\right]$$

Besides, the solid blue curve in Fig. 3 represents the "theoretical" fatigue life in PWR water, as predicted by Equation 2 by considering the F_{en} factor.

Equation 2 $$N_{PWR,\,theo}=\frac{N_{mean,\,air}}{F_{en,\,theo}} = \frac{\exp[6.891-1.92\times\ln(\Delta\varepsilon t/2-0.112)]}{F_{en,theo}}$$

In this equation, $F_{en,\,theo}$ is the theoretical value of the abatement factor on the fatigue life in PWR water. Several empirical models based on extended experimental databases have been established to predict its value [20-24]. According to the calculation method proposed in the latest NUREG report [20], for a strain rate of 0.4% s^{-1} and a temperature of 300°C, the $F_{en,\,theo}$ factor takes a value of 1.94.

In Fig. 3, the experimental fatigue life in PWR water is presented in blue solid circles. An experimental value of environment factor $F_{en,exp}$ can be derived from these data according to the equation and results are shown in Fig. 4. Given the limited set of data obtained in the course of the present study and in an attempt to take into account the scatter, a so-called semi-empirical value $F_{en,semi-exp}$ was also estimated by considering the equation below. The theoretical value $F_{en,\,theo}$ is indicated in Fig. 4 as well for comparison purpose.

Equation 3 $$F_{en,\,semi\text{-}exp} = \frac{N_{mean,\,air}}{N_{exp,\,PWR}} = \frac{\exp[6.891 - 1.92 \times \ln(\Delta\varepsilon t/2 - 0.112)]}{F_{en,theo}}$$

It can be seen in Fig. 4 that, for a total strain amplitude ranging between 0.2% and 0.5%, the $F_{en,exp}$ value ranges between 2.27 and 3.23, that means a higher value than the $F_{en,\,theo}$ value equal to 1.94. A harmful effect of the PWR water on the fatigue life is hence confirmed. For a total strain amplitude less than 0.2% however, $F_{en,exp}$ varies between 0.38 and 1.25. The effect of PWR water on the fatigue life is therefore not clear in this strain amplitude interval, and the method proposed in the latest NUREG report [20] tends to overestimate the deleterious effect of PWR water in this region. Furthermore, it has to be noticed that the influence of specimen geometry (solid versus hollow samples) on this tendency is extremely limited.

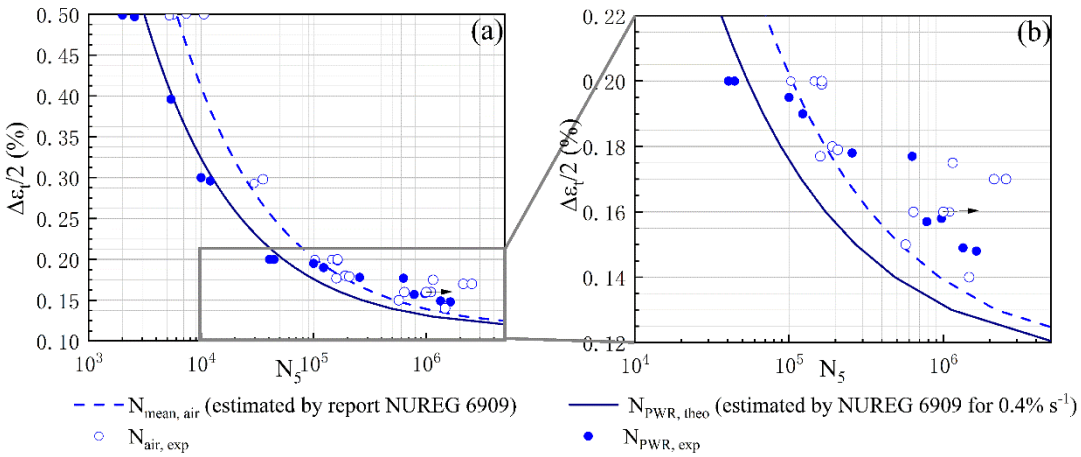

Fig. 3 : Fatigue life in air and PWR water environment, without mean stress. (a) For strain amplitude between 0.1% and 0.5%. (b) Enlargement of (a) for total strain amplitudes below 0.2% (arrow: run-out test).

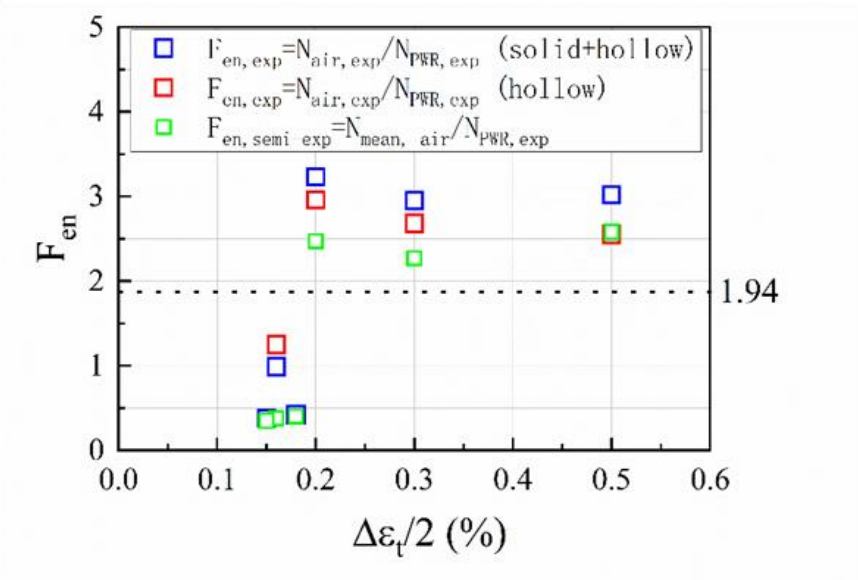

Fig. 4 : Estimation of the experimental environment factor $F_{en,exp}$,and semi-experimental $F_{en,semi-exp}$ as a function of total strain amplitude without mean stress.

3.2. Fatigue behavior with mean stress application

For tests with mean stress application, a tri-modal monitoring method is applied while the strain amplitude and the strain rate are fixed. An example of such a monitoring is given in Fig. 5 for a strain amplitude of 0.2%, and a mean stress of 20 MPa: the mean strain of the material (red curve) is automatically incremented by the closed-loop system of the test machine, so as to compensate the stress relaxation resulting from cyclic loading and to gradually increase the mean stress until reaching the setpoint value (green curve). The phase during which the mean stress is progressively increasing until reaching the set point is noted in the following as the transient stage. The duration of this transient stage depends on the imposed loading (strain rate, strain amplitude and mean stress level) and the monitoring parameters (PID and tri-modal

gain). In a previous research on 304 THY SS, at $\Delta\varepsilon_t/2$ = 0.18%, with a test frequency of 5 Hz (3.6%s^{-1}), the mean stress of 50 MPa could be reached by this tri-modal monitoring in several tens of cycles [18, 25], and at the end of the transient stage the mean strain is approximately zero at room temperature [18] but reached up to 2% at 300°C [25], using the same test rig. In this work, after optimization of PID and tri-modal gain settings, the transient stage was controlled in order to be less than 10% of the total fatigue life, i.e. about 200 cycles for a mean stress of 20 MPa, and 1000 cycles for mean stress of 50 MPa respectively; the mean strain reached at the end of the transient stage is approximately 0.75% for 20 MPa and 4.5% for 50 MPa (Fig. 6 (b)). The large mean strain level reached is due to the enhanced ductility and reduced strain-hardening with higher temperature [26-28].

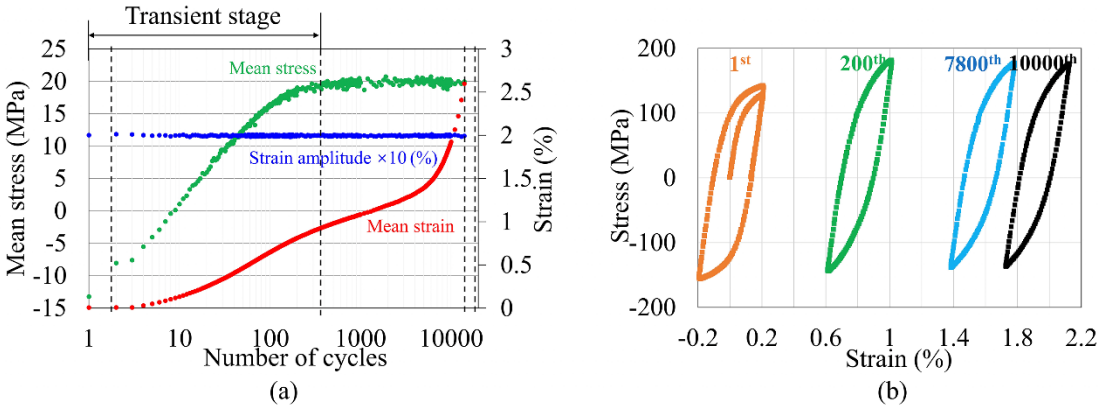

Fig. 5 : Example of the fatigue behavior with mean stress application in tri-modal monitoring mode ($\Delta\varepsilon_t/2$ = 0.2%, σ_m=20 MPa, in PWR water, fatigue life is 15600 cycles). (a) Evolution of the stress and strain in function of number of cycles. (b) Cyclic hysteresis loops of different number of cycles indicated by dotted black line in (b)

In Fig. 6, the cyclic stress-strain response of the material for a strain amplitude of 0.2% with different mean stress levels is shown to assess the impact of applied mean stress. It is observed that this tri-modal monitoring causes as expected an increase in mean stress (Fig. 6 (a)), but also in maximum stress (Fig. 6 (c)), as well as in mean strain (Fig. 6 (b)). Moreover, the amplitude of plastic strain decreases with the application of a mean stress, especially at 50MPa (Fig. 6 (d)). This is related to the fact that the total strain amplitude is controlled as constant while the stress amplitude increases during the fatigue test.

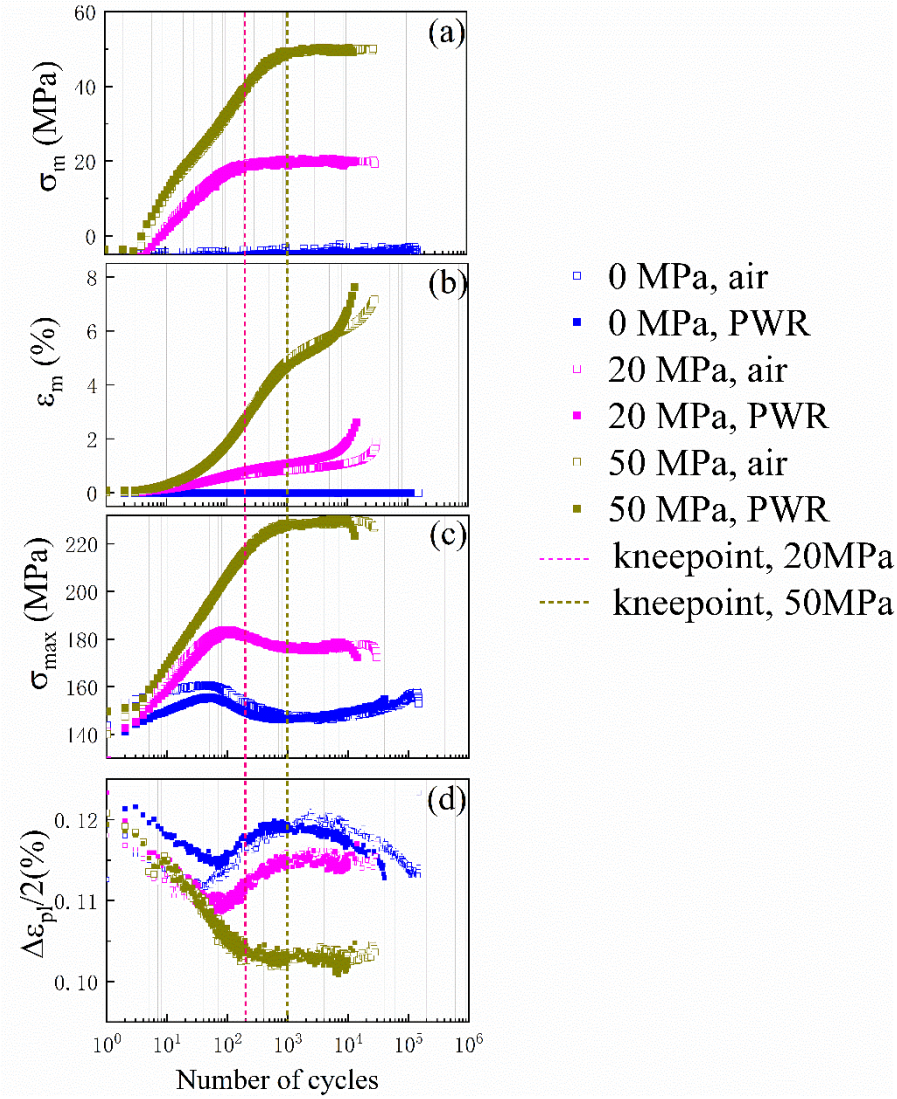

Fig. 6 : Cyclic stress-strain response in air and PWR water, $\Delta\varepsilon_t/2$ = 0.2%, at 0.4% s^{-1}, with different mean stress levels. (a) Evolution of mean stress, (b) Evolution of mean strain, (c) Evolution of maximum stress, (d) Evolution of plastic strain amplitude.

The effect of mean stress on fatigue life in air and in PWR water is presented in Fig. 7. For strain amplitudes varying from 0.14% to 0.2%, it can be seen that fatigue life is reduced when applying a mean stress of 20 MPa or 50 MPa as compared to tests under same conditions but without mean stress application. This reduction can be described by means of the F_{ms} factor defined as the ratio of the fatigue life without mean stress and the fatigue life with a mean stress in a given environment, as indicated in Fig. 7.

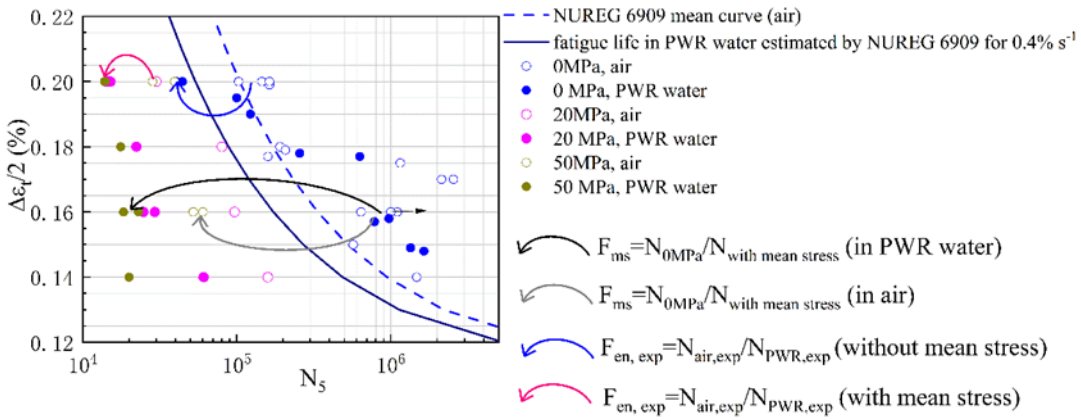

Fig. 7 : Fatigue life in air and in PWR water environment, with or without mean stress.

3.3 Fatigue crack initiation and growth stages at $\Delta\varepsilon_t/2 = 0.2\%$

The previous sections have presented results on the fatigue life obtained for total strain amplitudes varying from 0.14% to 0.5%. In this part, a focus is placed on the strain amplitude of 0.2% by analyzing additional data derived from interrupted tests carried out in air and in PWR water, without or with a mean stress of 50 MPa along with the results of tests conducted until failure. The objective is to evidence a possible joint effect of the mean stress application and of the exposure to PWR water on the fatigue crack growth process. With this aim, the maximum depth of the main crack observed on the fracture surface is firstly measured. Fig. 8 (a)-(e) show the measurements of crack depth for tests without mean stress application in air, at different number of cycles. The results for all tests in air and in PWR water, with and without

mean stress of 50 MPa are assembled and plotted as a function of the number of cycles in Fig. 8 (f).

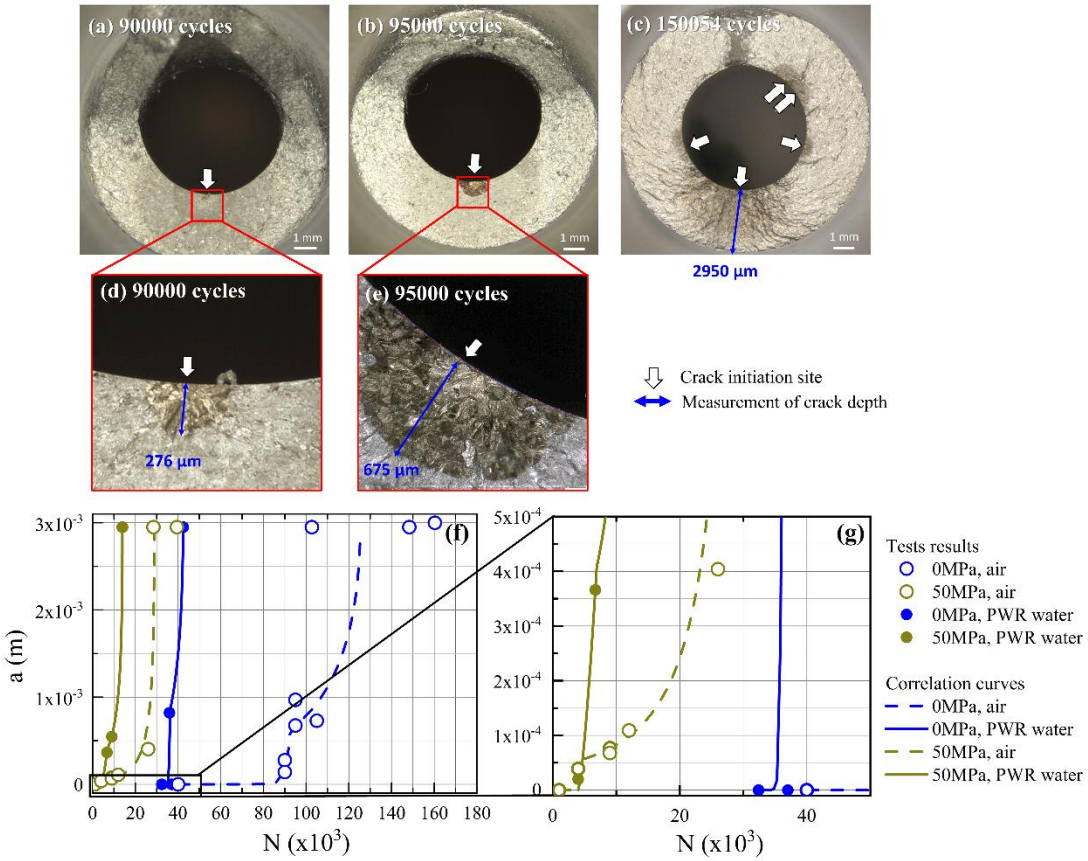

Fig. 8 : Fracture surface of the specimens after different number of cycles. 0 MPa. $\Delta\varepsilon_t/2$=0.2%. In air. (a) 90000 cycles. (b) 95000 cycles. (c) 150054 cycles (until rupture). (d) and (e) are magnifications of (a) and (b). (f) Fatigue crack propagation data derived from interrupted test and fitting curves

The fitting curves presented in Fig. 8 (f) were obtained by integrating the fatigue crack growth rates described by a Paris–Erdogan-type equation [29] expressed as a function of the strain intensity factor range ΔK_ε (Equation 4). The use of this parameter was proposed by Kamaya et al. [30, 31] for austenitic stainless steels and was used in previous research of the same material in similar test conditions [10, 32, 33].

Equation 4 $$\frac{da}{dN} = C \times \Delta K_\varepsilon{}^m$$

Here, C and m are parameters that depend not only on material properties, but also on additional factors such as environment, strain rate etc. Their values were here determined by a trial-and-error method, so as to fit the experimental curves obtained with hollow specimens (data obtained with solid specimens are not considered so as to eliminate any possible geometry impact on the crack propagation).

In order to achieve a satisfactory fitting to the experimental data, it was found necessary to consider two sets of parameters (C_1, m_1) and (C_2, m_2), corresponding with two regimes separated by a transition at a given number of cycles N_t, and at a transition depth of a_t. The values of C, m, N_t and a_t for each investigated condition are assembled in Table 3. This transition in crack growth rate was previously observed in 304 stainless steel on striation spacing as on crack growth rates derived from Direct Current Potential Drop (DCPD) monitoring method, at diverse strain amplitudes and strain rates and in different media [6, 34-36]. This can be attributed to a lower sensitivity to ΔK_ε (or crack depth) during the propagation of short cracks than the macro-crack propagation, firstly reported as a "short-crack" effect [37]. Except for the case with mean stress application in air, a_t is comprised from 200 μm to 900 μm, which is consistent with the threshold crack depth for the transition from a "Physically short crack" to a "Long crack" regime as suggested by Ould Amer [38] in 304 stainless steel.

Table 3 : Values of the parameters of the fatigue crack growth equations and the number of cycles at the transition for the experimental conditions under consideration.

Condition	C_1	m_1	N_t	a_t (μm)	C_2	m_2
0 MPa, air	1.55×10^{2}	2.22	91363	590	2.32×10^{2}	2.86
0 MPa, PWR	1.55×10^{2}	2.14	36000	821	1.10×10^{3}	2.62
50 MPa, air	7.36×10^{2}	2.40	3027	55	8.36×10^{3}	3.00
50 MPa, PWR	2.74×10^{-5}	0.55	7000	412	5.29×10^{5}	3.30

The numbers of cycles required to make a surface crack grow to a certain depth are then calculated by using these values represented by the fitting curves in Fig. 8 (f). In some previous research with $\Delta\varepsilon_t/2$=0.6%, 10-20 μm is frequently applied to define the depth of fatigue crack initiation for the 316 stainless steels [39] and for the investigated material [6, 40]. However, at $\Delta\varepsilon_t/2$=0.2%, even after 50% of the fatigue life, a considerable proportion of cracks can be stopped by the first grain boundaries encountered [38]. In fact, cracking remains sensitive to local microstructural barriers until a certain depth, known as the effect of short cracks [6, 32, 37, 38]. In this work, for most of observed fracture surfaces, the depth of the deepest crack, when existing, are no smaller than 77 μm, except one case showing only one crack of 39 μm. It has to be noted that the average grain size of the investigated material, measured by EBSD characterization on a statistic amounts of grains [6, 19, 40], is 80 μm.

Hence, based on statements and observations mentioned above, values of the depth of an initial crack a_0 as 10, 80 and 250 μm was separately considered, to estimate the crack initiation life and crack propagation life. By using the fitting curves in Fig. 8 (f), $Na_0 \rightarrow 2950\mu m$ is the number of cycles required to make a crack grow from a_0, to a final depth of 2950 μm, which is the wall thickness of the hollow specimen. The number of cycles $N_0 \rightarrow a_0$ required to nucleate a crack of

a_0 is thereafter derived by subtracting to the number of cycles to failure N_5. The result is shown in Fig. 9.

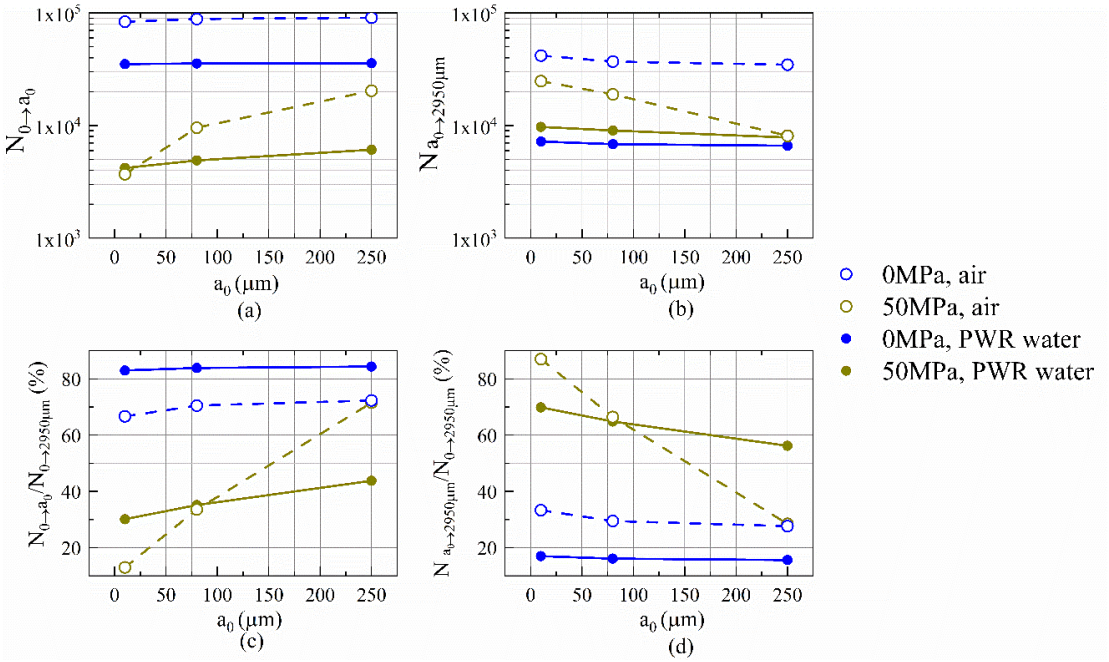

Fig. 9 : (a) Fatigue crack initiation life $N_{0\rightarrow a0}$ (b) fatigue propagation life $N_{a0\rightarrow 2950\mu m}$ (c) percentage of crack initiation life in total fatigue life. (d) percentage of crack propagation life in total fatigue life for different values of a_0 at $\Delta\varepsilon/2 = 0.2\%$.

Fig. 9 (a) and (b) share the same axis scale. One can note that the crack initiation life is generally in the same order of, or even higher than the crack propagation life, for the various values of a_0 considered. Without any applied mean stress (blue curves in Fig. 9), the propagation stage corresponds with less than one third of the total life. With mean stress application, the crack initiation life is greatly reduced (brown curves in Fig. 9 (c)), from more than 65% of the total fatigue life to less than 30%, if considering a_0 of 10µm and 80µm.

Focusing on Fig. 9, by comparing the hollow blue curve for air and the solid blue curve for PWR water, one can confirm the deleterious effect of the PWR environment in crack initiation stage and in crack propagation stage in the absence of mean stress. Besides, this effect of PWR environment during both crack initiation and propagation stage shows very little dependency on the value of a_0 considered. By comparing the blue dotted curve and the brown dotted curve, a negative effect of mean stress application in air for the crack initiation and propagation stage can be noticed. This negative effect during the crack initiation stage is

particularly pronounced while considering a_0 as 10 μm. However, when these two deleterious parameters co-exist, an interesting point is observed , indicated by brown solid curves in Fig. 9: the crack initiation life in PWR water with mean stress application is closed to that in air with mean stress application, if considering a_0 =10μm; the crack propagation life in PWR water with mean stress application is, on the other hand, slightly longer than the crack propagation life in PWR water but without applied mean stress, for all the considered values of the initial crack depth a_0.

4. Discussion

4.1. Effect of PWR water on fatigue life

From Fig. 8 (f) and Fig. 9 (a), it is revealed that this crack initiation life is much lower in PWR water than in air. This detrimental effect of PWR water on the crack initiation stage is in agreement with previous research [40-42].

Despite this enhancement of fatigue crack initiation in PWR water, the crack initiation stages in air and in PWR present some similarities. The first one is the predominance of the crack initiation life within the entire fatigue life in both environments in the absence of mean stress, as mentioned above. In fact, $N_{0\rightarrow a0}$ detains approximately 70% and 83% of the fatigue life, in air and in PWR water respectively, as shown in Fig. 9. It is worth noticing that the higher fraction in PWR water results from higher fatigue crack growth rates, and consequently a relatively shorter crack propagation stage, as it will be explained in the next section. The second similarity between the two environments lies in the nature of the crack initiation sites, which are generally related to surface defects introduced during specimen machining, as illustrated in Fig. 10 (a) to (d). In fact, Persistent Slip Bands (PSBs) are rarely observed on the surface, even at the end of the fatigue test, which can be at least partly attributed to the low values of plastic strain encountered in this domain. The third similarity is the limited number of crack initiation sites in both environments. The crack density, measured on the specimen internal surface (Fig. 10 (a) to (d)) and expressed in cracks/mm^2, and on cross sections of the sample (Fig. 10 (e) and (f)) and expressed in cracks/mm, are assembled in Fig. 10 (g). Only the specimens fatigued to failure are included in this plot, as the specimens from interrupted tests show only a very limited number of cracks: for instance, in air, only one crack is observed after 95000 cycles (69% of the fatigue life); in PWR water, only one crack is noticed after 36000 cycles (84% of the fatigue life); for another specimen tested to 37000 cycles in PWR water, no crack is detected. With a strain amplitude of 0.2%, crack density on the specimens tested to failure is low, in air as well

as in PWR water, while with a strain amplitude of 0.6%, the crack initiation site density is doubled in PWR water and reaches 23 mm^{-2} after just 600 cycles [6].

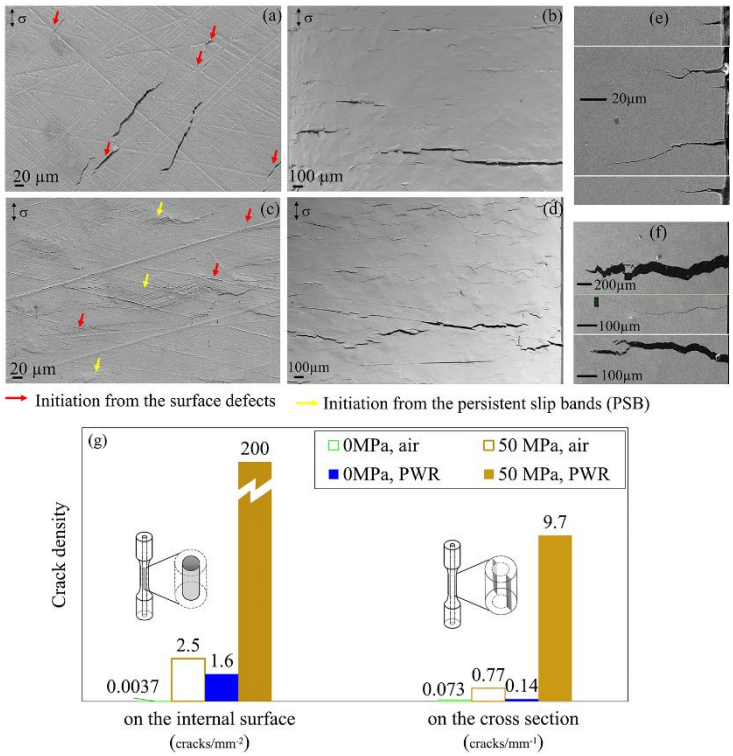

Fig. 10 : Observations of the cracks in the hollow specimens with a strain amplitude $\Delta\varepsilon_t/2$=0.2% after fatigue tests of different numbers of cycles. (a) 40731 cycles, without mean stress, in PWR water, on the internal surface. (b) 9000 cycles, 50 MPa, in air, on the internal surface. (c) (d) 9000 cycles, with a mean stress of 50 MPa, in PWR water, on the internal surface. (e) 40731 cycles, without mean stress, in PWR water, on cross section. (f) 15534 cycles, with a mean stress of 50 MPa, in PWR water, on cross section. (g) Crack density on the internal surface and on the cross section at the end of the fatigue test.

These similarities between the two environments suggest that, under a strain amplitude of 0.2%, and without any applied mean stress, the cyclic plastic strain accumulation represents the key factor controlling crack initiation. In air, a previous study carried out at higher strain amplitudes pointed out that cracks principally initiate from the extrusion/intrusions on the surface due to emergence of persistent slip bands [6, 19, 43]. In the present study however, due to the low strain amplitudes considered, the plastic strain accumulation is extremely slow, so that only very few slip bands are activated and emerged on the free surface. As a consequence, cracks preferably initiate in the vicinity of surface defects, where a local concentration of stress and/or deformation develops due to the geometry singularity. The PWR water environment can facilitate the crack initiation by successive repetition of oxidation of the strain concentration site, and rupture of the oxide film formed on the crack tip, as previously pointed out [19, 44]. Nevertheless, it is worth noticing that these interactions are based on the assumption of a

sufficient accumulation of plastic strain required to promote preferential oxidation [19, 43, 45] and to conduct to the failure of the oxide layer by shearing [43, 44].

Secondly, as concerns the crack propagation life as quantified by the $N_{a0\rightarrow 2950\mu m}$ parameter, the PWR water evidently reduces the crack propagation life, as indicated in Fig. 9 (b). This is furthermore consistent with the variation observed in fatigue striation spacing on the crack propagation area of the fracture surface, and, as presented in Fig. 11 as a function of ΔK_{ε}. In Fig. 11, the results for strain amplitudes equal to and lower than 0.2% are compared with results previously obtained for the same material and under the same strain rate, but at significantly higher strain amplitudes (0.6% [6, 40], 0.5% [19], and 0.3% [40]). It is found that, for a given environment (air or PWR water), the effect of strain amplitude on fatigue crack growth rates is extremely limited, and that the fatigue crack growth rate in air is always smaller than in PWR water. This suggests that, as long as the crack propagates in a stage-II mode along with the formation of fatigue striations, the harmful effect of PWR water is similar, regardless the applied strain amplitude varying from 0.14% to 0.6%. The fatigue crack growth equations established by Kamaya et al. [46, 47](curves in Fig. 11) present a fair estimation of the fatigue crack growth rates in air and especially in PWR water. However, it has to be pointed out that the positive mean stress and the associated progressive mean strain are expected to influence crack closure effects, but also the magnitude of environmental effect. Indeed, in a previous study, it was established that the crack is fully open with a slightly negative strain during the rising load part of a push-pull loading (R_{ε}=-1) [33]. As the magnitude of environmental enhancement of fatigue crack growth rate is controlled by the duration of exposure to environment, it is partly controlled by the opening strain. This effect is particularly marked at very slow strain rates. In the present study, the experimental conditions considered do not vary enough to distinguish any potential effect of the variation of the opening strain on fatigue crack growth rate enhancement in PWR environment. Indeed, the maximum factor on exposure duration is two.

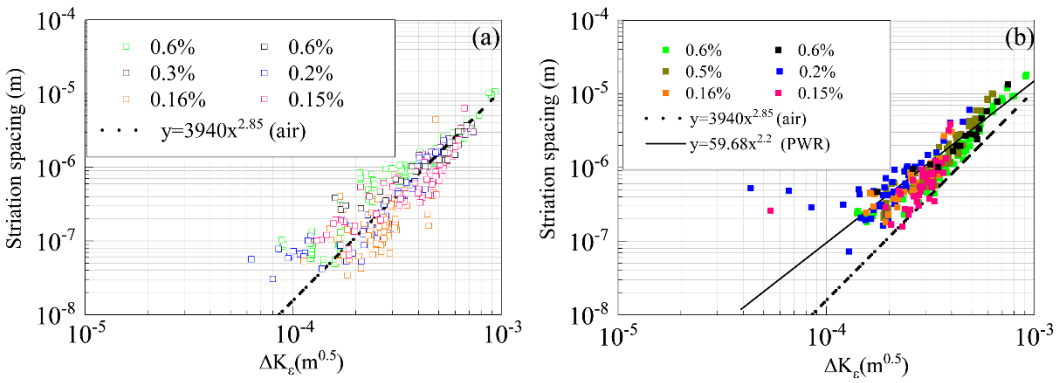

Fig. 11 : Striation spacing in function of ΔK_ε, without mean stress, at 0.4%s^{-1} in comparison with results at strain amplitudes of 0.6%[6, 40], 0.5% [19], and 0.3% [40]. (a) In air. (b) In PWR water.

The analysis developed in the two previous paragraphs, on crack initiation and crack propagation respectively, explains the drop in fatigue life noticed in PWR water at $\Delta\varepsilon_t/2$=0.2% without mean stress application, as shown by the pink arrow in Fig. 7. Besides, it provides a possible explanation for the disappearance of the negative effect of PWR water on fatigue life noticed in Fig. 3 and Fig. 4 for strain amplitude smaller than 0.2%. During the major part of the fatigue life at low strain amplitudes, the oxide layer on the specimen surface might not fail and the underlying metal is probably not exposed to the PWR water. As a consequence, during this period, the PWR environment might not significantly contribute to the crack initiation process. However, once the fatigue crack grows deep enough to form observable fatigue striations, the PWR effect is activated. However, as the crack propagation stage is relatively short compared to the initiation stage, the impact of PWR environment on the total fatigue life, which is represented by the $F_{en,exp}$ parameter, is very limited. Therefore, for such strain amplitudes typically lower than 0.2%, the $F_{en,exp}$ value is approximately equal to 1, while it is above 2 for strain amplitudes higher than 0.2%.

Besides, a negative effect of PWR water on the fatigue life is observed in Fig. 7 even for strain amplitudes varying from 0.14% to 0.2%. The threshold value of 0.2% for the strain amplitude established in the absence of mean stress application does no longer hold. A possible explanation for this is given in section 4.2.

4.2. Effect of mean stress on fatigue life

As shown in Fig. 6, the application of a mean stress greatly modifies the cyclic stress-strain response of the material, which in turn results in changes in the crack initiation mechanism. Firstly, the application of a mean stress leads to a sharp increase in crack density. Indeed the SEM observations of the internal surface of specimens indicate that, with a mean

stress of 50 MPa, a large quantity of PSBs are already formed on the internal surface of the specimens fatigued after 9000 cycles (Fig. 10 (c) (d)). The crack density measured on the internal surface and the cross section is significantly higher than the case without mean stress application, as shown in Fig. 10 (d). In contrast to the case without mean stress application, the defects initially present at the surface do no longer constitute the main crack initiation sites. Meanwhile, it can be seen from Fig. 9 (a) that the crack initiation stage is greatly reduced to about 35% of the total fatigue life, i. e. a much lower fraction compared to the case without mean stress application (about 80%). It is deduced that, for strain amplitudes smaller than 0.2%, the predominance of the crack initiation stage on the fatigue life does no longer hold with the application of mean stress. The mean stress application would thus favor the initiation of surface cracks, which are then exposed to the PWR water earlier during the fatigue life. This may be the reason for the negative effect of PWR water noticed with mean stress application for strain amplitudes lower than 0.2%.

The sharp increase in the number of PSBs indicates that the application of a mean stress under a given strain amplitude enhances the accumulation of plastic strain. It should be noted however that, in this study, the plastic strain amplitude decreases as a mean stress is applied (Fig. 6 (d)). Therefore, this enhancement of plastic strain accumulation should be attributed to the increase of maximum stress or the mean strain (Fig. 6 (a)-(c)). Further discussion on that point is provided in sections 4.5 and 4.6.

Besides, as regards the crack propagation stage, as indicated in in Fig. 9 (b), the harmful effect of the mean stress application in air is confirmed. In PWR water however, the mean stress application even shows a slightly beneficial impact. Considering the scatter in data, it is likely that, in PWR water, the mean stress application effect on crack propagation is either neutral or slightly positive. An in-depth investigation of the crack propagation micro-mechanism would be necessary to explain the disappearance of the mean stress effect in PWR water during the crack propagation stage.

4.3. Influence of mean strain on the fatigue life

In this study, the trimodal monitoring method induces an increase of the maximum stress, the minimum stress, the stress amplitude, and the mean strain. More particularly, the variation of the mean strain can be extremely important, typically up to 8% at the end of the tests with a mean stress of 50MPa and a strain amplitude of 0.2%. The potential role of such a mean strain in the reduction of fatigue life under mean stress application is discussed in the following lines.

Firstly, previous researches on polished specimen made from pre-hardened austenitic stainless steel show that, for a given strain amplitude, the mean strain level does not lead to

reduction of fatigue life in air [14, 48] nor in PWR water [15, 49]. These studies however concerned pre-straining from 10% to 40%, that means largely higher than the mean strain values achieved here. Therefore, it can be deduced that, in the tests presented here, the mean strain by itself is not responsible for the fatigue life reduction. It is the modification of the mean strain, characterized by the ratcheting strain, or the modification in surface roughness that may have potential negative effect on the fatigue life.

In stress-controlled tests carried out on a non-prestrained 316L austenitic stainless steel [49], even though the ratcheting strain increases, it was observed that the fatigue life was improved with the applied mean stress. This indicates that the cyclic hardening outweighs the possible detrimental effect of positive ratcheting strain on fatigue life. However, the analysis of ratcheting strain as generated by the trimodal control used in this study was not examined in previous studies.

In this study, the ratcheting strain $\Delta\varepsilon_r$ is defined as the difference between the mean strain measured at 10% of the fatigue life and the one measured at 95% of the fatigue life, as expressed in *Equation 5*. The mean strain variation prior to crack initiation and the one occurring near the final rupture are therefore excluded in this definition. The choice of the 10% of the fatigue life as a lower bound for this parameter is furthermore consistent with the transient regime shown in Fig. 5 corresponding to the establishment of the imposed mean stress.

Equation 5 $$\Delta\varepsilon_r=\varepsilon_{m,\ 95\%\ of\ the\ fatigue\ life} - \varepsilon_{m,10\%\ of\ the\ fatigue\ life}$$

In Fig. 12 (a), the decrease in fatigue life due to the application of mean stress, expressed as the difference between the reference fatigue life in absence of mean stress $N_{0MPa,average}$ and the fatigue life resulting from the application of a mean stress N: $N_{0MPa,average}–N_5$, is plotted as a function of $\Delta\varepsilon_r$. $N_{0MPa,average}$ was determined for each environment and strain amplitude, by averaging all the obtained reference fatigue tests results. It comes out that, for a fixed strain amplitude, the decrease in fatigue life induced by the application of a mean stress can be considered as independent of the ratcheting strain value. In Fig. 12 (b), the reduction of fatigue life is described by the ratio $N_5/N_{0MPa,average}$. Without mean stress application, $N_5/N_{0MPa,average}$ in PWR water varies from 0.7 to 1.3, which represents an index of the scatter in the fatigue lives in the absence of mean stress. The reference value of the ratio $N_5/N_{0MPa,average}$ is expected to be around 1 but as it can be seen in Fig. 12 (b) it is characterized by a relatively large scatter, especially in air. Nevertheless, it is shown that in the presence of a mean stress, the ratio $N_5/N_{0MPa,average}$ is significantly lower than 1, but does not seem to be affected by the ratcheting strain nor by the environment. Hence, a mean value around 0.3 is obtained with a strain amplitude of 0.2%, and less than 0.1 at lower amplitudes, almost regardless of the test environment.

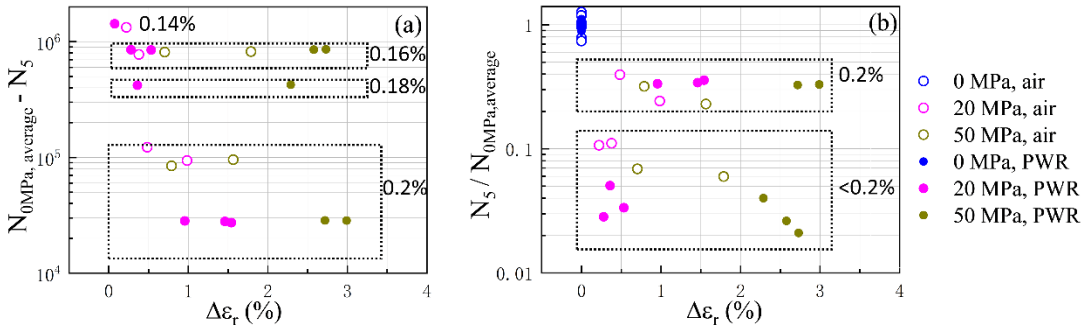

Fig. 12 (a) decrease of fatigue life due to the application of a mean stress $N_{0MPa,average}$-N_5 in function of the ratcheting strain $\Delta\varepsilon_r$ (2) Normalized fatigue life with or without mean stress $N_5/N_{0MPa,average}$ as a function of the ratcheting strain $\Delta\varepsilon_r$

Kamaya and Kawakubo [48] carried out fatigue tests with a mean stress application on a 316L austenitic stainless steel in air at room temperature and calculated a normalized fatigue life by considering the life determined by the effective strain range, that means the range during which the crack is fully open, as a function of the ratcheting strain. The inverse correlation between these two parameters was explained by the authors by the fact that a high value ratcheting strain favors the crack opening and therefore enhances the crack growth rates. However, in another research on 316L SS in air but at 300°C [15], the relation between this normalized life and the ratcheting strain is no longer obvious, but is characterized by a considerable scatter, in agreement with the tendency presented here. It is therefore likely that ratcheting does contribute to the reduction in fatigue life in presence of a mean stress application, for example by enhancing the crack opening as explained in [14, 15, 48], but at high temperature, this influence tends to saturate when a small ratcheting value, typically less than 0.5% in the present study, is achieved. This is probably why a similar weak dependence on the ratcheting strain is observed in PWR water in this study. Further investigation of this suggestion is nevertheless required.

Given that, it can be concluded that ratcheting, despite of the high mean strain value that can be achieved at the end of test, is of limited contribution in the fatigue life reduction due to mean stress application, particularly in PWR water.

5. Conclusions

This paper reported on experimental results of uniaxial strain amplitude-controlled fatigue tests carried out to get insight into the joint influence of the exposure to PWR water and of the application of a mean stress on the fatigue strength of a 304L austenitic stainless steel,

with a special attention paid to the strain amplitudes equal or smaller than 0.2%. The main findings can be summarized as follows.

1. In the absence of mean stress application, for a strain amplitude ranging between 0.2% and 0.5%, the fatigue life in PWR water is reduced as compared to air. The experimental environmental factor F_{en} in this regime lies between 2.27 and 3.23, that means slightly higher than the theoretical value of 1.94 derived from the NUREG/CR-6909 report [20] for this condition.
2. Furthermore, it is shown that the reduction in fatigue life induced by PWR water is related to the acceleration of the crack initiation stage, as well as of the crack propagation stage. For a strain amplitude smaller than 0.2%, the PWR water effect on fatigue life is negligible, as the crack initiation stage predominates the entire fatigue life under such loading conditions and as the PWR water has only a limited impact during this stage. However, additional fatigue tests at small strain amplitudes below 0.2%, and with other strain rate below $0.4\%s^{-1}$ are still necessary to definitively assess this point.
3. With a given strain amplitude lying between 0.14% and 0.2%, the application of a tensile mean stress reduces the fatigue life by accelerating the crack initiation stage and the crack propagation stage in air, but merely by accelerating the crack initiation stage in PWR water. An in-depth investigation of the crack propagation micro-mechanism would be necessary to explain the disappearance of the mean stress effect in PWR water during the crack propagation stage.
4. Due to the enhancement of the plastic strain accumulation induced by the mean stress application, the crack initiation stage is accelerated and the PWR water effect on fatigue life is re-activated for strain amplitude below 0.2%, in the presence of a mean stress.

Declaration of Competing Interest

The authors declare that they have no known competing financial interests or personal relationships that could have appeared to influence the work reported in this paper.

CRediT authorship contribution statement

Z. Peng: Investigation, writing original draft & editing. G. Henaff: Supervision, discussion, writing review & editing. J-C. Le Roux: Investigation, writing - review & editing. R. Verlet: Investigation, writing - review & editing.

Acknowledgement

This work has been funded by the MODERN project of EDF (2017-2020), under the contract between EDF and ENSMA (n° EDF 5920049526). All the fatigue tests and

experimental analysis in this work were conducted in EDF R&D Laboratory Site des Renardières.

References

1. (2010) Boiler and Pressure Vessel Code, ASME, 2010. ASME.
2. (2009) Règles de Conception et de Construction des Matériels Mécaniques des Ilots Nucléaires REP.
3. Metais T, Courtin S, Genette P, De Baglion L, Gourdin C, Le Roux JC (2015) OVERVIEW OF FRENCH PROPOSAL OF UPDATED AUSTENITIC SS FATIGUE CURVES AND OF A METHODOLOGY TO ACCOUNT FOR EAF. *ASME Pressure Vessels and Piping Conference, PVP-2015*. Amer Soc Mechanical Engineers, Boston, MA.
4. Higuchi M, Iida K (1991) Fatigue strength correction factors for carbon and low-alloy steels in oxygen-containing high-temperature water. *Nuclear Engineering and Design*. **129**: 293-306.
5. Bernardconnolly M, Buiquoc T, Biron A (1983) MULTILEVEL STRAIN CONTROLLED FATIGUE ON A TYPE-304 STAINLESS-STEEL. *Journal of Engineering Materials and Technology-Transactions of the Asme*. **105**: 188-194.
6. de Baglion L (2011) Comportement et endommagement en fatigue oligocyclique d'un acier inoxydable austénitique 304L en fonction de l'environnement (vide, air, eau primaire REP) à 300°C. 1 vol. (306 p.).
7. Nikitin I, Besel M (2008) Correlation between residual stress and plastic strain amplitude during low cycle fatigue of mechanically surface treated austenitic stainless steel AISI 304 and ferritic-pearlitic steel SAE 1045. *Materials Science and Engineering a-Structural Materials Properties Microstructure and Processing*. **491**: 297-303.
8. Petitjean S (2003) Influence de l'état de surface sur le comportement en fatigue à grand nombre de cycles de l'acier inoxydable austénitique 304L. IX-287 p.
9. KURODA M, MARROW TJ (2008) Modelling the effects of surface finish on fatigue limit in austenitic stainless steels. *Fatigue & Fracture of Engineering Materials & Structures*. **31**: 581-598.
10. Poulain T, Mendez J, Henaff G, de Baglion L (2017) Analysis of the ground surface finish effect on the LCF life of a 304L austenitic stainless steel in air and in PWR environment. *Engineering Fracture Mechanics*. **185**: 258-270.
11. Huin N, Couvant T, Legras L, Loisnard D, Mendez J, Henaff G (2012) Environmental effect on fatigue of austenitic stainless steels exposed to PWR Primary water. *ASME Pressure Vessels and Piping conference 2012*, Toronto, Canada.
12. Colin J, Fatemi A, Taheri S (2010) Fatigue Behavior of Stainless Steel 304L Including Strain Hardening, Prestraining, and Mean Stress Effects. *Journal of Engineering Materials and Technology-Transactions of the Asme*. **132**: 13.
13. Chen W, Spätig P, Seifert HP (2020) Role of Mean Stress on Fatigue Behavior of a 316L Austenitic Stainless Steel in LWR and Air Environments. *International Journal of Fatigue*. 106111.
14. Kamaya M (2017) MEAN STRESS EFFECT ON FATIGUE PROPERTIES OF TYPE 316 STAINLESS STEEL (PART I: IN HIGH-TEMPERATURE AIR ENVIRONMENT). *ASME Pressure Vessels and Piping Conference*. Amer Soc Mechanical Engineers, Waikoloa, HI.
15. Kamaya M (2017) MEAN STRESS EFFECT ON FATIGUE PROPERTIES OF TYPE 316 STAINLESS STEEL (PART II: IN PWR PRIMARY WATER ENVIRONMENT). *ASME Pressure Vessels and Piping Conference*. Amer Soc Mechanical Engineers, Waikoloa, HI.

16. Solomon HD, Amzallag C, Vallee AJ, De Lair RE, Asme (2005) Influence of mean stress on the fatigue behavior of 304L SS in air and PWR water. *Pressure Vessels and Piping Conference of the American-Society-of-Mechanical-Engineers*. Amer Soc Mechanical Engineers, Denver, CO, 87-97.
17. Poncelet M, Barbier G, Raka B, et al. (2010) Biaxial High Cycle Fatigue of a type 304L stainless steel: Cyclic strains and crack initiation detection by digital image correlation. *Eur J Mech A-Solids*. **29**: 810-825.
18. Vincent L, Le Roux JC, Taheri S (2012) On the high cycle fatigue behavior of a type 304L stainless steel at room temperature. *International Journal of Fatigue*. **38**: 84-91.
19. Huin N (2013) Environmental effect on cracking of an 304L austenitic stainless steels in PWR primary environtment under cyclic loading. ISAE-ENSMA Ecole Nationale Supérieure de Mécanique et d'Aérotechique - Poitiers.
20. Chopra OK, Stevens GL (2018) Effect of LWR Water Environments on the Fatigue Life of Reactor Materials, Final Report.
21. Hasegawa H (2011) Nuclear Power Generation Facilities—Environmental Fatigue Evaluation Method for Nuclear Power Plants. Japan Nuclear Energy Safety Organization.
22. Le Duff JA, Lefrancois A, Vernot JP (2009) EFFECTS OF SURFACE FINISH AND LOADING CONDITIONS ON THE LOW CYCLE FATIGUE BEHAVIOR OF AUSTENITIC STAINLESS STEEL IN PWR ENVIRONMENT COMPARISON OF LCF TEST RESULTS WITH NUREG/CR-6909 LIFE ESTIMATIONS. In: Rodery CD, ed. *Proceedings of the Asme Pressure Vessels and Piping Conference, Vol 3*, 453-462.
23. Chopra OK, Shack WJ (2007) Effect of LWR Coolant Environments on the Fatigue Life of Reactor Materials, Final Report.
24. Chopra OK, Stevens GL (2014) Effect of LWR Coolant Environments on the Fatigue Life of Reactor Materials, Draft Report for Comment.
25. Vincent L (2012) Essais de Fatigue à Grand Nombre de Cycles et à 300°C Sur Un Acier Inoxydable Austénitique AISI 304L: Premiers Résultats Sur l'effet d'une Contrainte Moyenne et d'une Déformation Moyenne. Commissariat à l'énergie atomique et aux énergies alternatives.
26. Byun TS, Hashimoto N, Farrell K (2004) Temperature dependence of strain hardening and plastic instability behaviors in austenitic stainless steels. *Acta Materialia*. **52**: 3889-3899.
27. Kim JW, Byun TS (2010) Analysis of tensile deformation and failure in austenitic stainless steels: Part I – Temperature dependence. *Journal of Nuclear Materials*. **396**: 1-9.
28. Soares GC, Rodrigues MCM, Santos LdA (2017) Influence of Temperature on Mechanical Properties, Fracture Morphology and Strain Hardening Behavior of a 304 Stainless Steel. *Materials Research*. **20**.
29. Paris PC, Erdogan F (1963) A critical analysis of crack propagation laws. *Trans ASME, J Bas Eng*. **85**: 528-534.
30. Kamaya M (2015) Low-cycle fatigue crack growth prediction by strain intensity factor. *International Journal of Fatigue*. **72**: 80-89.
31. Kamaya M, Kawakubo M (2012) Strain-based modeling of fatigue crack growth - An experimental approach for stainless steel. *International Journal of Fatigue*. **44**: 131-140.
32. Cussac P (2020) Influence d'imperfections surfaciques sur la tenue en fatigue de composants nucléaires.
33. Poulain T, de Baglion L, Mendez J, Hénaff G (2019) Influence of Strain Rate and Waveshape on Environmentally-Assisted Cracking during Low-Cycle Fatigue of a 304L Austenitic Stainless Steel in a PWR Water Environment. *Metals*. **9**: 197.
34. Cussac P, Gardin C, Pelosin V, et al. (2020) Low-cycle fatigue crack initiation and propagation from controlled surface imperfections in nuclear steels. *International Journal of Fatigue*. **139**: 105703.

35. Poulain T, Mendez J, Henaff G, De Baglion L (2016) Characterization of Damage During Low Cycle Fatigue of a 304L Austenitic Stainless Steel as a Function of Environment (Air, PWR Environment) and Surface Finish (Polished, Ground). *Procedia Engineering*. **160**: 123-130.
36. Poulain T, Mendez J, Hénaff G, de Baglion L (2014) Influence of the Strain Rate on the Low Cycle Fatigue Life of an Austenitic Stainless Steel with a Ground Surface Finish in Different Environments. In: Clark G, Wang CH, eds. *11th International Fatigue Congress, Fatigue 2014*. Advanced Materials Research, Melbourne, Australia, 1320-1326.
37. Suresh S (1991) *Fatigue of Materials*, Cambridge.
38. Ould-Amer A (2014) Endommagement à différentes échelles d'un acier austénitique inoxydable en fatigue à amplitude constante et variable. ENSTA, Palaiseau.
39. Mineur M, Villechaise P, Mendez J (2000) Influence of the crystalline texture on the fatigue behavior of a 316L austenitic stainless steel. *Materials Science and Engineering a-Structural Materials Properties Microstructure and Processing*. **286**: 257-268.
40. Poulain T (2015) Low Cycle Fatigue of a 304L Austenitic Stainless Steel : Influence of Surface Finish and Load Signals in PWR Water Environment. ISAE-ENSMA Ecole Nationale Supérieure de Mécanique et d'Aérotechique - Poitiers.
41. Chopra OK (2002) Mechanism and Estimation of Fatigue Crack Initiation in Austenitic Stainless Steels in LWR Environments.
42. Huin N, Tsutsumi K, Legras L, et al. (2012) *FATIGUE CRACK INITIATION OF 304L STAINLESS STEEL IN SIMULATED PWR PRIMARY ENVIRONMENT: RELATIVE EFFECT OF STRAIN RATE*. Amer Soc Mechanical Engineers, New York, 165-171.
43. Couvant T, Legras L, Herbelin A, et al. (2008) *Development of Understanding of The Interaction between Localized deformation and SCC of Austenitic Stainless Steels Exposed to Primary Environment*.
44. Ford FP (1992) Slip dissolution model. In: Desjardin D, Oltra R, eds. *Corrosion Sous Contrainte - phénoménologie et mécanismes*. les Editions de Physique, 307-344.
45. Legras L, A. Vogin B, Radiguet, B. , et al. (2017) Using microscopy to help with the understanding of degradation mechanisms observed in materials of pressurized water reactors. *Journal of Materials Science and Engineering B* **7**: 187-220.
46. Kamaya M (2013) Environmental effect on fatigue strength of stainless steel in PWR primary water - Role of crack growth acceleration in fatigue life reduction. *International Journal of Fatigue*. **55**: 102-111.
47. Kamaya M, Kawakubo M (2012) Damage Assessment of Low-Cycle Fatigue by Crack Growth Prediction (Development of Growth Prediction Model and Its Application). *TRANSACTIONS OF THE JAPAN SOCIETY OF MECHANICAL ENGINEERS Series A*. **78**: 1518-1533.
48. Kamaya M, Kawakubo M (2015) Mean stress effect on fatigue strength of stainless steel. *International Journal of Fatigue*. **74**: 20-29.
49. Spätig P, Heczko M, Kruml T, Seifert HP (2018) Influence of mean stress and light water reactor environment on fatigue life and dislocation microstructures of 316L austenitic steel. *Journal of Nuclear Materials*. **509**: 15-28.